Electrospun α-lactalbumin nanofibers for site-specific and fast-onset delivery of nicotine in the oral cavity

an in vitro, ex vivo and tissue spatial distribution study

Kalouta, Kleopatra; Stie, Mai Bay; Janfelt, Christian; Chronakis, Ioannis S.; Jacobsen, Jette; Mørck Nielsen, Hanne; Foderà, Vito

Published in:
Molecular Pharmaceutics

Link to article, DOI:
10.1021/acs.molpharmaceut.0c00642

Publication date:
2020

Document Version
Peer reviewed version

Article

Electrospun #-lactalbumin nanofibers for site-specific and fast-onset delivery of nicotine in the oral cavity: an in vitro, ex vivo and tissue spatial distribution study

Kleopatra Kalouta, Mai Bay Stie, Christian Janfelt, Ioannis S. Chronakis, Jette Jacobsen, Hanne Mørck Nielsen, and Vito Foderà

Mol. Pharmaceutics, **Just Accepted Manuscript** • DOI: 10.1021/acs.molpharmaceut.0c00642 • Publication Date (Web): 04 Sep 2020

Electrospun α-lactalbumin nanofibers for site-specific and fast-onset delivery of nicotine in the oral cavity: an *in vitro*, *ex vivo* and tissue spatial distribution study

Kleopatra Kalouta[1,a,b], Mai Bay Stie[1,a,b], Christian Janfelt[a], Ioannis S. Chronakis[c], Jette Jacobsen[a], Hanne Mørck Nielsen*[,a,b] and Vito Foderà*[,a,b]

[1] Co-first authors: Kleopatra Kalouta, Department of Pharmacy, University of Copenhagen, Universitetsparken 2, 2100 Copenhagen, Denmark & Mai Bay Stie, Department of Pharmacy, University of Copenhagen, 2 Universitetsparken, 2100 Copenhagen, Denmark

[*] Corresponding authors: Hanne Mørck Nielsen, Department of Pharmacy, University of Copenhagen, 2 Universitetsparken, 2100 Copenhagen, Denmark & Vito Foderà, Department of Pharmacy, University of Copenhagen, 2 Universitetsparken, 2100 Copenhagen, Denmark

[a] Department of Pharmacy, University of Copenhagen, 2 Universitetsparken, 2100 Copenhagen, Denmark

[b] Center for Biopharmaceuticals and Biobarriers in Drug Delivery, University of Copenhagen, 2 Universitetsparken, 2100 Copenhagen, Denmark

[c] DTU Food, Technical University of Denmark, Kemitorvet, B202, 2800 Kgs. Lyngby, Denmark

ABSTRACT

Nicotine replacement therapy (NRT) formulations for oromucosal administration induce a delayed rise in nicotine blood levels as opposed to the immediate nicotine increase obtained from cigarette smoking; this being a shortcoming of the therapy. Here, we demonstrate that α-lactalbumin/polyethylene oxide (ALA/PEO) electrospun nanofibers constitute an efficient oromucosal delivery system for fast-onset nicotine delivery of high relevance for acute dosing NRT applications. *In vitro*, nicotine-loaded nanofibers showed fast disintegration in water, with a weight loss up to 40% within minutes, and a faster nicotine release (26.1±4.6% after 1 min of incubation) of the loaded nicotine compared to two relevant marketed NRT formulations with a comparable nicotine dose (*i.e.* 7.9±5.1% and 2.2±0.3% nicotine was released from a lozenge and a sublingual tablet, respectively). Model-fitting of the release data indicated that the release mechanism of nicotine from the hydrophilic nanofibers was possibly governed by more than one type of release phenomena. Remarkably, *ex vivo* studies using porcine buccal mucosa demonstrated a more efficient permeation of the nicotine released from the nanofibers (flux of 1.06±0.22 nmol/(cm^2×min)) compared to when dosing even a ten-fold concentrated nicotine solution (flux of 0.17±0.14 nmol/(cm^2×min)). Moreover, MALDI MS imaging of *ex vivo* porcine buccal mucosa exposed to nicotine-loaded nanofibers clearly revealed higher amounts of nicotine throughout the epithelium, as well as in the lamina propria and submucosa of the tissue. Our findings suggest that nicotine-loaded ALA/PEO nanofibers have potential as a mucosal, fast-releasing and biocompatible delivery system for nicotine, which can overcome the limitations of current marketed NRTs.

KEYWORDS: Electrospun protein nanofibers; nicotine; nicotine replacement therapy; *in vitro* characterization; *ex vivo* tissue permeation; MALDI mass spectrometry imaging

INTRODUCTION

Tobacco smoking represents a public health issue and is one of the leading yet preventable mortality causes worldwide.[1] Every year, approximately 6 million deaths globally are attributed to diseases related to cigarette smoking.[2] Tobacco smoking strains the healthcare system and imposes a great economic burden on society.[2] The total annual financial cost of smoking, including the productivity losses from death and disability, accounts for more than US $1.4 trillion, which is equal to a 1.8% magnitude of the global annual Gross Domestic Product (GDP).[2] The harmful effects of tobacco smoking on human health are attributed to its toxic components such as carbon monoxide and tar constituents.[3] However, it is the principal tobacco alkaloid, nicotine, which acts as the neuroactive modulator of the psychopharmacological effects related to the addiction.[4,5] Nicotine is a small (MW 162.23 g/mol) diamine[6] ($pKa_{,1}$ 3.26 and $pKa_{,2}$ 7.9 at T=37°C),[7] which is highly soluble in aqueous media (water solubility between 33 and 100 g/L).[8]

Pharmacological and non-pharmacological interventions are recommended strategies for handling tobacco smoking addiction and succeeding in its cessation.[9] Nicotine replacement therapy and non-nicotine medication with e.g. bupropion and varenicline are examples of pharmacological approaches, and are recommended as first-line pharmacological treatment.[10] Non-pharmacological support can be provided by e.g. behavioral counselling.[9] Noteworthy, it has been shown that the combination of non-nicotine medication and NRT may represent a potential efficient approach.[9] By replacing the supply of nicotine from tobacco, NRT aids tobacco users in dealing with reinforcing effects induced by cigarette smoking such as cravings and other symptoms, e.g. irritability or sickness caused by nicotine abstinence,[11] and NRT thus facilitate the transition from cigarette smoking to complete cessation.[12,13]

The existing NRT products are generally well tolerated and demonstrate minor adverse effects.[14] Examples of oromucosally administered NRTs for acute dosing of nicotine comprise nicotine oral spray, chewing gums, oral films, lozenges, and sublingual tablets.[15–18] The sustained release NRTs, e.g. transdermal patches, mainly act as attenuators of background craving levels due to nicotine abstinence.[19]

Nonetheless, numerous challenges are linked to the use of NRTs. Primarily, current NRT formulations that are designed to be administered and absorbed in the oral cavity, do not trigger a physiological response comparable to the response obtained by cigarette smoking and absorption

of nicotine from the respiratory tract. The pharmacokinetics of nicotine upon release and absorption from the current formulations administered in the oral cavity are not as rapid as for nicotine absorbed from cigarettes.[3] This is due to the fact that the absorption of nicotine into the blood from such products is slower, reaches therapeutic levels later, and that a rapid systemic arterial delivery of nicotine is not achieved. This results in dissatisfaction and further cravings of smokers.[3] However, nicotine may be sufficiently absorbed into the systemic circulation through the buccal mucosa and examples of NRT formulations targeting this route of administration are e.g. the oral film,[20] chewing gum[21] and lozenge.[22] Unfortunately, significant amounts of nicotine may not be absorbed, but rather swallowed due to saliva flow, followed by extensive first pass metabolism yielding a low bioavailability of nicotine from these products.[5,20] Swallowed nicotine can eventually also lead to side effects such as gastrointestinal discomfort, nausea, throat soreness, and hiccups.[14] Moreover, specifically for the gum, nicotine is partially retained and not completely released from the formulation.[5] There is therefore a need for more fast-acting, effective and user-friendly NRT formulations, which can satisfy cravings and eventually inhibit smoking relapse to support smokers in coping with smoking cessation. For example, films and wafers with mucoadhesive properties have recently been under investigation as alternative buccal NRT delivery systems.[17]

An ideal delivery system for nicotine i) provides ease of self-administration, ii) is intended for e.g. buccal administration, from which site nicotine is efficiently absorbed, iii) disintegrates and facilitates fast nicotine release, and iv) provides a site-specific release of nicotine, thus ensuring a high concentration gradient and enhancing the passive diffusion of nicotine across the mucosa. Nanofibers produced by electrospinning have recently gained ground for numerous applications in areas such as wound healing, tissue engineering, and drug delivery.[23] This is mainly due to their high drug loading efficiency, tunability, adhesiveness to the site of application, high surface-to-volume ratio, and ability to control loading and release of molecules at the target site.[24] Proteins from plant or animal sources are exploited for various biomedical applications due to their structural and functional properties and biocompatibility.[25] For the current application, nanofibers were produced by waterborne electrospinning of the biocompatible and biodegradable[25,26] whey protein α-lactalbumin (ALA) with minute amounts of polyethylene oxide (PEO), as previously reported.[27] ALA is heat-stable, digestible,[28] a natural vehicle of essential micronutrients[26] and shown to have antibacterial[29] and anticancer properties.[30] The protein is a good source of the

essential amino acid tryptophan, which is related to the human ability to cope with stress.[31] Moreover, ALA-based nanofibers are hydrophilic, scalable and highly tunable, and the protein maintains its native structural characteristics after electrospinning.[27]

The objective of the current study was to investigate ALA/PEO nanofibers as a potential NRT formulation for oromucosal administration. Here, we report on ALA/PEO nanofibers loaded with a content of nicotine comparable to that of marketed NRT formulations. The nicotine-loaded nanofibers showed a faster release of nicotine than existing NRTs *in vitro*. Nicotine released from the nanofibers successfully permeated across filter-grown TR146 cell culture epithelium *in vitro* and through *ex vivo* porcine buccal mucosa. Remarkably, the nicotine from the nanofibers penetrated throughout the buccal mucosa and surpassed the epithelial permeability barrier. We demonstrate the potential of ALA/PEO nanofibers as a delivery system for site-specific release of nicotine leading to fast permeation of high amounts of drug. The nanofiber-based delivery system is comparable to marketed NRT formulations in terms of the content of nicotine, but superior in terms of the drug delivery efficiency.

MATERIALS & METHODS

Materials

ALA (92.5% purity) was kindly provided by Davisco Food International/Agropur Ingredients (Eden Prairie, MN, USA). Nicotine was used in the form of nicotine bitartrate dihydrate (NBT), which was kindly donated by Fertin Pharma A/S (Vejle, Denmark). Nicotinell® 1 mg mint Lozenge (GlaxoSmithKline, Brentford, Middlesex, UK) and NICORETTE® Microtab (McNeil Products, Maidenhead, UK) were purchased through the Association of Danish Pharmacies. PEO (MW 300 kDa), Hanks' Balanced Salt Solution (HBSS), phosphate buffer saline (PBS) pH 7.4, glycerol, sucrose, L-glutamine, penicillin, streptomycin, phenazine methosulfate (PMS), Dulbecco's Modified Eagle's Medium high-glucose (DMEM), 2,5-dihydroxybenzoic acid (DHB), Mayer's hematoxylin solution, alcoholic eosin Y solution, potassium phosphate dibasic, phosphoric acid (85%), sodium hydroxide, bovine serum albumin (BSA) and the TR146 cell line were purchased from Sigma Aldrich (St. Louis, MO, USA). N-2-hydroxyethylpiperazine-N'-2-ethanesulfonic acid (HEPES) was obtained from PanRec AppliChem (Damstadt, Germany). Fetal bovine serum (FBS) was obtained from PAA laboratories (Brøndby, Denmark). Acetonitrile (99.9%) and absolute ethanol (99.97%) were purchased from VWR Chemicals BDH® International (Leicestershire, UK). 3-(4,5-dimethylthiazol-2-yl)-5-(3-carboxymethoxyphenyl)-2-(4-sulfophenyl)-2H-tetrazolium) (MTS) was obtained from Promega (Madison, WI, USA). Methanol was purchased from Th. Geyer (Renningen, Germany). Ultrapure water was collected in-house (18.2 MΩ×cm by a PURELAB flex 4 system, ELGA, LabWater, High Wycombe, UK).

Methods

Production of nicotine-loaded ALA/PEO nanofibers

ALA/PEO nanofibers were produced by electrospinning using the method previously described.[27] Briefly, a 37.5 %(w/w) solution of ALA in ultrapure water was mixed in a 1:1 (w/w) ratio with a 7.4 %(w/w) PEO dispersion in ultrapure water. The mixed dispersion was stirred for at least 30 min prior to electrospinning. Subsequently, the dispersion was electrospun at room temperature (20±2 °C) with a high voltage supply of 15-16 kV (Gamma High Voltage Research, Ormond Beach, FL, USA), a flow rate of 1 mL/h (New Era Pump Systems, Farmingdale, NY, USA), a relative humidity under 30% (secured by flow of dry air) and a tip-collector distance of 15 cm from a 5 mL syringe with a 20 G blunt needle. Assuming total evaporation of the aqueous solvent, nanofibers with a final content of 84 %(w/w) ALA and 16 %(w/w) PEO were produced. The

investigated formulation comprised five stacked nanofiber discs cut from the electrospun nanofiber mat by using an aluminum puncher with a diameter of 11 mm. 15 µL of nicotine in absolute ethanol (15 mg/mL) was applied on each of the discs dropwise, and the nanofiber discs were layered in the aluminum puncher-container used for cutting (Figure S1, Supporting Information). Slight wetting of the nanofibers by the nicotine in ethanol solution facilitated the adherence of the five discs into one while the ethanol evaporated. The final formulation (nicotine-loaded nanofibers) had a diameter of 11 mm, an average weight of 19.33±2.89 mg (N=3, n=7; mean ± SD, where N equals the number of different nanofiber mats prepared on different days and n the number of samples weighed per mat), and carried a theoretical load of 1.125 mg nicotine.

Morphological and *in vitro* characterization of the nicotine-loaded ALA/PEO nanofibers

Morphological analysis and size evaluation

The ALA/PEO nanofibers and the nicotine-loaded nanofibers were morphologically characterized by scanning electron microscopy (SEM). Visualization of the nanofibers was performed under a Phenome Pro X scanning electron microscope (Pheno-World, Eindhoven, Netherlands) at an accelerated voltage of 15 kV. The samples were mounted on aluminum SEM stubs with carbon tape and sputter-coated with gold. The diameters of the nanofibers were measured using the IMAGE J software version 1.52h (National Institute of Health, Bethesda, MD, USA) and results were averaged for samples produced on two different days. The diameter of 150-300 individual fibers were measured for each sample. For statistical comparison of the diameters of ALA/PEO nanofibers and nicotine-loaded nanofibers, a two-tailed unpaired t-test with equal variances was employed with prior comparison of variances in the groups by application of statistical analysis by an F-test.

Disintegration study

A disintegration study in water was conducted for nicotine-loaded nanofibers with an average weight of 19.33±2.89 mg (N=3, n=7; mean ± SD). Samples of nicotine-loaded nanofibers were weighed ($m_{initial}$), placed in 11 mm aluminum baskets with holes, submerged in 3 mL ultrapure water, and incubated at 37 ^{o}C for 1 h with mild agitation (50 rpm) according to previous reports.[32] Samples were withdrawn at specific time points (1, 5, 10, 20, 30, 45, and 60 min), the containers were gently blotted on paper to remove excess water and the remaining nanofibers were left to dry

until constant weight (m_{final}) was reached. Weight loss was determined by the following equation (Eq. 1):

$$\text{Weight loss} = \frac{m_{initial} - m_{final}}{m_{initial}} \times 100\% \quad \text{(Eq. 1)}$$

The results were averaged for samples prepared on three different days, cut out of three different nanofiber mats, prepared on three different days.

Nicotine release profile *in vitro*

Final formulations of nicotine-loaded nanofibers and non-loaded nanofibers (i.e. fibers treated with an ethanol solution without nicotine) were investigated for release of nicotine. A 2 mg nicotine sublingual tablet, with nicotine in the form of nicotine bound to cyclodextrin (NICORETTE® Microtab), and a 1 mg nicotine lozenge, with nicotine in the form of NBT salt (Nicotinell® 1 mg mint Lozenge), were used for comparison. The different samples were submerged in 3 mL 10 mM HEPES in HBSS (hHBSS) pH 6.8 in a 12-well plate, with all nanofiber samples placed in an aluminum container with holes. Subsequently, the samples were incubated at 37 °C with mild agitation at 50 rpm. 100 µL aliquots of each sample were taken at different time points (1, 5, 10, 20, 30, 45, 60 and 120 min), and replaced with 100 µL hHBSS pH 6.8. The aliquots were centrifuged (10,621 ×g, 8 min, 4 °C) and the release of nicotine was quantified by reversed phase high performance liquid chromatography (RP-HPLC) using a prominence system (Shimadzu, Kyoto, Japan) with a C18 (150×4.6 mm; 5 µm) column (Phenomenex, Værløse, Denmark) fitted with a security guard cartridge (4×3 mm) (Phenomenex) and a mobile phase (15:85 (v/v)) of acetonitrile:dipotassium phosphate 20 mM (pH 8.5; adjusted with phosphoric acid) with a flow rate of 0.8 mL/min, an injection volume of 10 µL, and isocratic elution. UV signals were measured with a PDA detector (SPD-M20A-Shimadzu, Kyoto, Japan) at 254 nm. The method was validated using nicotine standards in hHBSS pH 6.8 and nicotine concentrations ranged from 0.4 $\times 10^{-3}$ mg/mL to 0.7 mg/mL (R^2=0.99). The peak area was used, and the limit of detection (LOD) was <32 ng/mL. Using OriginPro 2019, the initial phase of the release profile (corresponding to approximately 60% released nicotine) was fitted to three different mathematical drug release models, presented in Table 1, where F is the fraction (%) of nicotine released in time (min).[33,34] The Hixson-Crowell model was only used to fit the release data obtained with the lozenge and the sublingual tablet, since it is

only relevant for modeling the release profile of pharmaceutical formulations such as tablets, for which the surface decreases proportionally over time and the geometrical form is maintained.[33]

Table 1. Release models fitted to the *in vitro* nicotine release data for the nicotine-loaded nanofibers, lozenge and sublingual tablet. F is the fraction (%) of nicotine released over time (min). The Hixson-Crowell model was only used to fit the release data obtained with the lozenge and sublingual tablet.

Release model	Equation
1st order	$F = 100 \cdot \left(1 - e^{-k_1 \cdot t}\right)$ (Eq.2), k_1: 1st order release constant
Korsmeyer-Peppas for burst effect	$F = F_0 + k_{KP} \cdot t^n$ (Eq.3), F_0: fraction of nicotine released at t=1 min, k_{KP}: Korsmeyer-Peppas release constant, n: release exponent, indicating the mechanism of nicotine release
Hixson-Crowell	$F = 100 \cdot [1 - (1 - k_{HC})^3]$ (Eq.4), k_{HC}: Hixson-Crowell release constant

Subsequently, in order to determine the model that fitted best to the release data obtained with each formulation, the Akaike information criterion (AIC)[35] was applied. AIC was calculated by the following equation (Eq.5):

$$AIC = n \times \ln(RSS) + 2 \times p \text{ (Eq. 5)}$$

, where n is the number of data points, RSS is the residual sum of squares and p is the number of parameters in each model. The model with the lowest AIC value was chosen as the best fit.

The nicotine release study was performed three times for nanofibers punched out of three different nanofiber mats prepared on three different days. Commercial products (lozenge and sublingual tablet) were from the same batch.

Evaluation of the nanofibers as a drug delivery system to facilitate permeation of nicotine

Nicotine transport across buccal TR146 epithelium and viability of cells

The *in vitro* permeation of nicotine across buccal TR146 epithelium was analyzed as previously described by Nielsen *et al.*.[7] TR146 cells were cultured in Corning Costar® polystyrene culture flasks (175 cm^2, Sigma Aldrich, St. Louis, MO, USA) in DMEM supplemented with FBS (10 %(v/v), L-glutamine (2 mM), penicillin (100 U/mL) and streptomycin (100 µg/mL) in a humidified environment at 37 °C with 5% CO_2. 4.3×10^5 TR146 cells were seeded on permeable Falcon® inserts (4.2 cm^2, pore size 0.4 µm) and cultured for 14 days. The cells were initially visualized

under a Leica DM IL LED microscope (Brønshøj, Denmark). The cells were washed twice; each time by adding 750 µL and 1.5 mL warm hHBSS pH 7.4 to the apical and the basal cell side, respectively. Subsequently, the cells were cooled to RT and the initial transepithelial electrical resistance (TEER) was measured using a resistance chamber (Endohm, World Precision Instruments, Sarasota, FL, USA) connected to a voltmeter (EVOM, World Precision Instruments, Sarasota, FL, USA). On the apical side, the cells were either exposed to 750 µL hHBSS pH 6.8 (control), ALA/PEO nanofibers submerged in 750 µL hHBSS pH 6.8, nicotine-loaded ALA/PEO nanofibers submerged in 750 µL hHBSS pH 7.4 (end pH ~6.8 as the bitartrate decreased the pH) or 0.3 mg/mL nicotine in 750 µL hHBSS pH 7.4 (end pH ~6.8 as the bitartrate decreased the pH). 0.3 mg/mL nicotine equals the theoretical concentration of nicotine released from the nanofibers. The inserts were quickly transferred to a new plate with 1.5 mL hHBSS pH 7.4, 0.05 %(w/v) BSA on the basal side of all inserts to initiate the experiment. The cells were incubated for 3 h at 37 °C with mild agitation at 50 rpm. Samples of 100 µL were withdrawn from the basal side of the inserts at different time points (15, 30, 45, 60, 90, 120, 150, and 180 min) and replaced with 100 µL of hHBSS pH 7.4, containing 0.05 %(w/v) BSA. The aliquots were centrifuged (10,621×g, 8 min, 4 °C) and analyzed by RP-HPLC as described in the method for nicotine release. The accumulated amount of nicotine, Q (mmol) transported from the apical to the basal side of the epithelium was determined. Q/A, where A=0.9 cm^2 the cross-sectional area of the tissue, was plotted as a function of time (min). The steady-state flux J_{SS} (mol/(cm^2×s)) is the slope of the linear part of these curves, and the lag time is the intercept of each of the linear equations with the x-axis. For the nicotine solution, the apparent permeability (P_{app}) for nicotine under sink condition was calculated by the following equation (Eq. 6) utilizing the relevant concentration of nicotine in the test sample (C_{donor}):

$$P_{app} = \frac{J}{C_{donor}} \quad \text{(Eq. 6)}$$

After 3 h of incubation, the pH and osmolality of samples withdrawn from the basal and the apical side of the epithelium were determined. The epithelium was washed twice with hHBSS pH 7.4, cooled to RT and the TEER was measured. The corrected TEER values were calculated by the following equation (Eq. 7):

$$TEER = (R_{insert\ with\ cells} - R_{insert\ without\ cells}) \times A \quad \text{(Eq. 7)}$$

, where $R_{insert\ with\ cells}$ is the resistance of the TR146 epithelium on the inserts and $R_{insert\ without\ cells}$ is the background resistance measurement of the inserts without cells.

The viability of the epithelial cells after exposure was evaluated using the MTS/PMS colorimetric assay. The epithelium was again warmed to 37 °C, the buffer was aspirated, 500 µL MTS/PMS solution was added to the apical side and 1.5 mL hHBSS pH 7.4 was added to the basal side. For the MTS/PMS assay, the final concentration of PMS was 1.2 µg/mL and the concentration of MTS was 120 µg/mL in hHBSS pH 7.4. Subsequently, the cells were incubated at 37 °C with mild agitation at 50 rpm for 40 min to 1 h. Finally, four aliquots of 80 µL were transferred to a transparent 96-well plate and the absorbance was measured at 492 nm (Abs_{sample}) in a plate reader spectrophotometer (POLARstar OPTIMA, BMG LABTECH, Ortenberg, Germany) and the relative cell viability was calculated by the following equation (Eq. 8):

$$\text{Relative cell viability (\%)} = \frac{Abs_{sample} - Abs_{blank}}{Abs_{control} - Abs_{blank}} \times 100\% \quad \text{(Eq. 8)}$$

, where Abs_{blank} is the absorbance of the unreacted MTS/PMS solution at 492 nm and $Abs_{control}$ is the absorbance of the control sample at 492 nm.

The transport study was performed on three cell passages for nanofibers punched out of three different nanofiber mats prepared on three different days.

Ex vivo permeation of nicotine through porcine buccal mucosa in Ussing chambers

The *ex vivo* permeation study of nicotine through porcine buccal mucosa was analyzed as previously described by Nielsen *et al.*.[7] *Ex vivo* buccal tissue was obtained from healthy experimental Danish Landrace/Yorkshire x Durox (D-LY)) pigs (of approximately 30 kg), and stored at -80 °C in cryo-medium (40 %(w/v) glycerol and 20 %(w/v) sucrose in PBS pH 7.4).[36] Initially, the porcine buccal mucosa was gently thawed in PBS in an ice bath with mild agitation to remove the cryo-medium. The mucosal tissue was trimmed with surgical scissors and finally cut with a Stadie-Riggs tissue slider (Thomas Scientific, Swedesboro, NJ, USA) to a thickness of 759±104 µm (N=3, n=2-3; mean ± SD) as determined by a manual micrometer. Then, the buccal mucosa was mounted in Ussing sliders P2413 (Physiologic Instruments, San Diego, CA, USA) with a 0.71 cm^2 exposure area. Nicotine-loaded nanofibers were placed on the buccal mucosa and fixed in place with Parafilm to ensure unidirectional release. The sliders were secured in Ussing

chambers (Physiologic Instruments, San Diego, CA, USA), with the epithelium facing the donor chamber. 2.0 mL PBS with 0.05 %(w/v) BSA was added in the receptor chamber. 2.0 mL of 5.625 mg/mL nicotine in PBS (pH 3.28 due to the influence of tartaric acid) was added on the donor side of the chambers without nanofibers (control samples). 5.625 mg/mL nicotine is equal to 10× the theoretical concentration of nicotine released from the nanofibers. Samples of 100 µL were taken from the receptor chamber at different time points (1, 15, 30, 45, 60, 90, 120, 150, 180, 210, 240, 270, and 300 min) and replaced with equal amounts of PBS containing 0.05 %(w/v) BSA. Donor samples were taken from the control samples at the beginning and at the end of the experiment. The samples were centrifuged (10,621 ×g, 8 min, 4 ^{o}C) and analyzed by the RP-HPLC method described above. Flux values for each of the samples and permeability for the nicotine solution were calculated using the method described in the transport study. Throughout the experiment, the temperature was kept at 37±2 ^{o}C and hydrated atmospheric air was supplied for stirring. The *ex vivo* study was performed three times on tissue obtained from three individual pigs. Six nicotine-loaded nanofibers samples from three different nanofiber mats were used.

MALDI mass spectrometry (MS) imaging and hematoxylin and eosin (H&E) staining with visualization by microscopy

For MALDI MS imaging, *ex vivo* porcine buccal mucosa was trimmed using surgical scissors to an approximate thickness of 3 mm, and placed in an Ussing chamber slider (area 0.71 cm^2; P2413; Physiologic Instruments, San Diego, CA, USA) with the nicotine-loaded ALA/PEO nanofibers and Parafilm as described in the *ex vivo* methods section above. The porcine buccal mucosa was exposed to the nicotine-loaded nanofibers under the same conditions as used for the *ex vivo* experiment above, but the experiment was terminated after 1 h of incubation. At the end of the incubation, the nanofibers were gently removed from the buccal tissue, and the tissue was placed in aluminum foil at -80 °C. Cryo-sectioning, matrix application and MALDI MS imaging were performed using the method described by Marxen *et al.*.[8] Briefly for imaging, as previously described,[8] the analysis was performed on a Thermo QExactive Orbitrap mass spectrometer (Thermo Fisher Scientific, Bremen, Germany) equipped with the AP-SMALDI10 Ion source (TransMIT Gesellschaft für Technologietransfer, Gieβen, Germany) with a mass range of m/z 150−800 in positive ionization mode. The mass resolving power was 140,000@m/z 200 and the m/z 295.02131 signal of the DHB matrix was used as a lock mass to ensure a mass accuracy of 2

ppm. Images with a pixel size of 20 μm were acquired. Raw data were converted to imzML files and visualized in MSiReader software version 0.09[37] (5 ppm bin width). Subsequently, 96 %(v/v) ethanol was used to wash off the matrix from the tissue section, which was then stained with hematoxylin and eosin (H&E) as described by Janfelt *et al.*[38] and imaged under a light microscope (Olympus, Tokyo, Japan) equipped with the AxioCam ERc5s camera (Zeiss, Jena, Germany). The experiment was performed twice for nanofibers punched from two different nanofiber mats prepared on two different days and on *ex vivo* buccal tissue from two individual pigs.

RESULTS & DISCUSSION

Morphology of nicotine-loaded ALA/PEO nanofibers

Unique characteristics of electrospun nanofibers such as high drug loading capacity and large surface area[39] have previously motivated electrospinning of the whey protein ALA into uniform, beadless nanofibers for drug delivery applications.[27] Properties of ALA, such as stability, biocompatibility and, most importantly, its high water solubility across a wide pH range[28] raised the hypothesis that depositing nicotine on electrospun ALA/PEO nanofibers could result in a promising fast onset nicotine delivery system for buccal administration. In accordance with previously obtained results,[27] ALA/PEO nanofibers demonstrated an average diameter of 646±110 nm (N=2, n=300; mean ± standard deviation (SD)). Nicotine was deposited onto the ALA/PEO nanofibers via a 5-layer method in an amount comparable to marketed NRT formulations (1.125 mg nicotine) (Figure S1). The nicotine-loaded ALA/PEO nanofibers appeared less flexible and more fragile than the neat ALA/PEO nanofibers after visual examination (Figures 1A/top-left and 1B/top-left), but not to an extent that limited handling. Nicotine-loaded nanofibers maintained a fibrous, entangled structure after deposition of nicotine (Figure 1B/top-right). The average diameter of the nicotine-loaded nanofibers (692±134 nm) (N=2, n=150; mean ± SD) (Figure 1B/bottom) was significantly higher ($p<0.0001$) than the diameter of the neat ALA/PEO nanofibers (646±110 nm) (N=2, n=300; mean ± SD) (Figure 1A/bottom). This could be explained by swelling of the nanofibers after exposure to the ethanol solution.

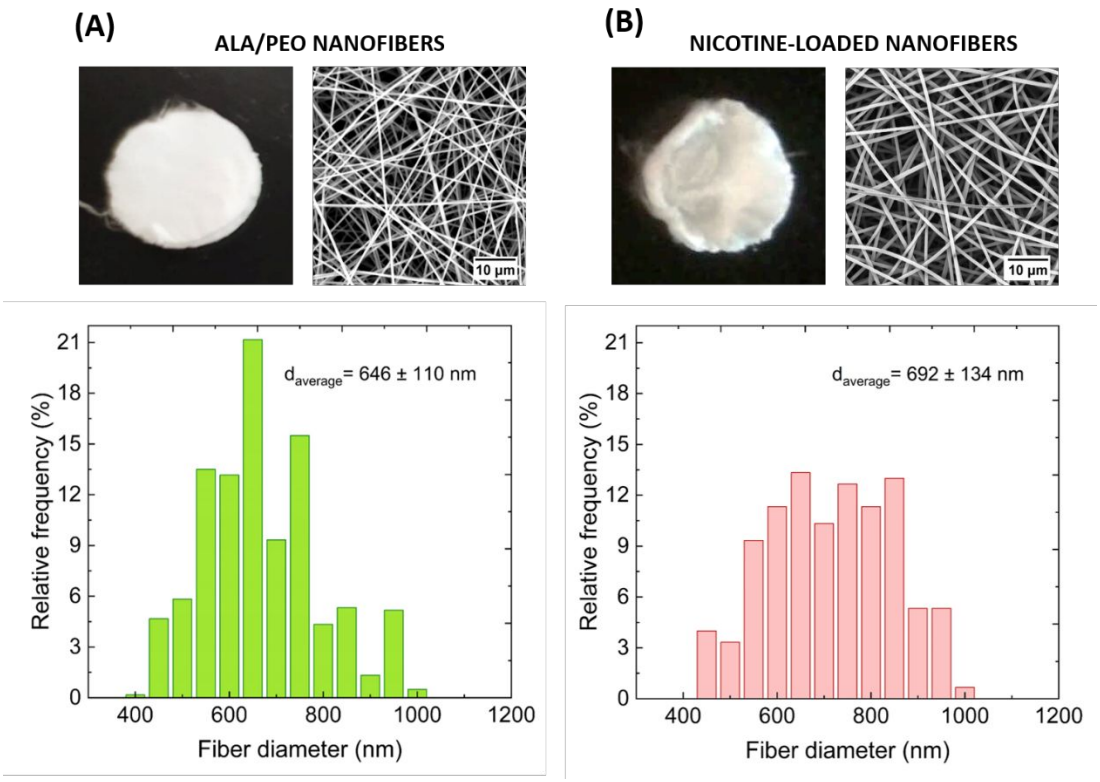

Figure 1. Characterization of nicotine-loaded nanofibers. (A) Disc of neat ALA/PEO nanofibers with a diameter of 11 mm (top-left), representative SEM image of the samples (top-right) and relative frequency (%) of the diameters of nanofibers (bottom). (B) Disc of nicotine-loaded ALA/PEO nanofibers with a diameter of 11 mm (top-left), representative SEM image of the sample (top-right) and relative frequency (%) of the diameters of nicotine-loaded nanofibers (bottom). N=2, n=150-300, N representing the number of nanofiber mats prepared on separate days and n the number of measured diameters per sample.

Nicotine-loaded nanofibers disintegrated quickly in aqueous media

The disintegration of nicotine-loaded ALA/PEO nanofibers in water was further evaluated and, as expected, a significant weight loss was detected for the nanofibers upon exposure to water (Figure 2). In accordance with previous findings, the hydrophilicity of ALA and PEO led to instant disintegration of the ALA/PEO nanofibers upon exposure to an aqueous medium.[27] Nicotine-loaded ALA/PEO nanofibers also demonstrated a rapid disintegration with up to 40% weight loss within minutes and only remnants of nanofibers observed by the end of the study. In total, a loss of more than 80% of their initial weight was observed within 1 h (Figure 2). This confirms that the intrinsic hydrophilic nature of the components of the nicotine-loaded nanofibers (ALA, PEO and nicotine) was maintained.[6,28] Interestingly, the nicotine-loaded nanofibers did not fully disintegrate after 1 h, probably due to the acidic environment created by the tartaric acid salt of NBT,[40] which could have altered the disintegration properties of the nanofibers in aqueous medium. The buffer

hHBSS pH 6.8 (salivary pH)[41] is more physiologically relevant than water in maintaining pH and being isoosmolal. However, for practical reasons water was chosen as the disintegration medium to avoid the additional weight due to deposition of salts from the buffer on the nanofibers after drying.

In general, electrospun hydrophilic nanofibers have been investigated as potential drug delivery systems for rapid release of deposited drugs.[42] Designed to be instantly wetted by saliva, they disintegrate fast, directly release and deliver the loaded drug into e.g. the buccal mucosa for immediate systemic absorption.[42] For instance, a study conducted on polyvinyl pyrrolidone (PVP) electrospun nanofibers loaded with the non-steroidal anti-inflammatory drug ketoprofen indicated that hydrophilic nanofibers display higher drug loading and faster drug release as opposed to that observed from hydrophobic nanofibers based on ethyl cellulose and cellulose acetate.[43]

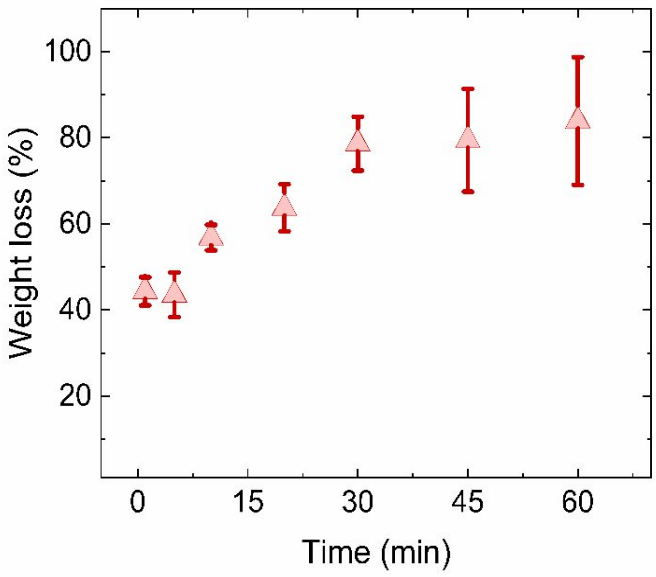

Figure 2. Disintegration of nicotine-loaded nanofibers of an average weight of 19.33±2.89 mg in 3 mL ultrapure water. N=3, N representing the number of different nanofiber mats prepared on different days. Results presented as the mean ± SD.

Nicotine-loaded nanofibers demonstrated a more rapid and efficient release profile compared to two marketed NRTs

The *in vitro* release profile of nicotine from the nanofibers was compared to the release profile of two marketed NRTs for oromucosal administration: a sublingual tablet and a lozenge. The sublingual tablet and the lozenge were chosen as these are acute dosing NRTs for rapid nicotine release and are for administration in the oral cavity. Via our deposition method, the nicotine-loaded

nanofibers had a nicotine content comparable to these marketed NRTs. Figure 3 represents the cumulative release of nicotine in percent of the total loaded amount of nicotine in the three formulations evaluated (1.125 mg, 1 mg, or 2 mg in the nanofibers, the lozenge, or the sublingual tablet, respectively). The release study was conducted for 2 hrs to investigate the complete release of nicotine from the nanofibers. 94.3±5.9% (N=3, mean ± SD) of the nicotine deposited on the ALA/PEO nanofibers was released within 2 h of incubation. A faster rate of nicotine release is observed for the nicotine-loaded nanofibers compared to that of the marketed formulations (Figure 3, highest rate constant in Table 2). Already after 1 min of incubation, 26.1±4.6% (N=3; mean ± SD) of the loaded nicotine was released from the nanofibers as opposed to only 7.9±5.1% (N=3; mean ± SD) and 2.2±0.3% (N=3; mean ± SD) nicotine released from the lozenge and the sublingual tablet, respectively. After 1 h, 89.1±5.9% (N=3; mean ± SD) of the loaded nicotine was released from the nanofibers, while 32.5±8.5% (N=3; mean ± SD) and 77.0±19.7% (N=3; mean ± SD) of the loaded nicotine was released from the lozenge and the sublingual tablet, respectively.

Most of the nicotine loaded onto the nanofibers was expected to be at or near the surface of the nanofibers, which could explain the faster release of nicotine. Also, with the deposition method used for this formulation, nicotine was expected to be weakly associated to the drug delivery system or adsorbed on its large surface area and thus display a rapid release.[44] Accordingly, previous studies on an oral fast-dissolving nanofibrous delivery system of caffeine and riboflavin showed that the molecular characteristics, the dispersed state and the solubility of the incorporated drugs in the formulation significantly influenced the release of the drugs.[45] In contrast, probably due to differences in the excipients and type of formulation (e.g. cyclodextrin bound nicotine in the sublingual tablet), the sublingual tablet and lozenge showed a slower release rate of nicotine in comparison to the nanofibers.[44] In accordance with the obtained results, previous release tests on patented and marketed lozenges with a USP dissolution Apparatus 1 at 100 rpm in phosphate buffer pH 7.5 claimed no more than 50% release of nicotine after 1 h of dissolution test.[46] The slow release of nicotine from the lozenge could partially be explained by the fact that the *in vivo* suction action was not simulated sufficiently in the current experimental setup. As also stated by a previous study on nicotine release from chewing gums, the evaluation of the performance requires suitable chewing apparatus to simulate the masticatory action.[47] Noteworthy, in contrast with other NRT formulations, the nanofibers were designed to be wetted by saliva, disintegrate and release nicotine

instantaneously towards the buccal mucosa by being easily administered i.e. without requiring efforts of the user such as chewing or suction.

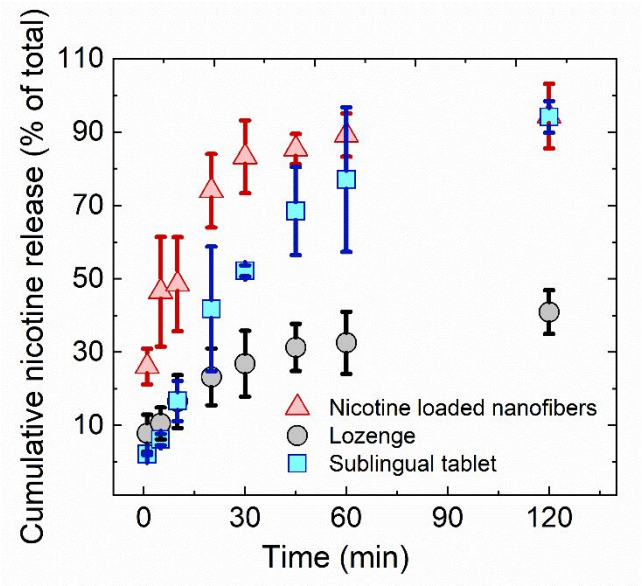

Figure 3. *In vitro* release profile of nicotine from nicotine-loaded nanofibers (1.125 mg nicotine), lozenge (1 mg nicotine) and sublingual tablet (2 mg nicotine). The cumulative amount of released nicotine calculated relative to the total amount of loaded nicotine of each formulation as a function of time. N=3, N representing the number of nanofiber mats prepared on different days, presented as the mean ± SD.

To further investigate the release of nicotine from the three types of formulations, the release data were fitted to three mathematical drug release models: the 1st order kinetics model (Figure S2A, Supplementary Information), the Korsmeyer-Peppas model for the case of a burst initial release effect (Figure S2B, Supplementary Information) and the Hixson-Crowell model (Figure S2C, Supplementary Information).[33,34] The kinetic parameters, the R^2 values and the AIC values obtained from fitting the data to the three models and application of (Eq. 5) are presented in Table 2. R^2 values were high ($R^2 \geq 0.962$) for all, except for the release data obtained with the sublingual tablet when fitted to the Korsmeyer-Peppas model for burst effect ($R^2=0.753$). R^2 values ($R^2 \geq 0.962$) indicated a good fit of the release data obtained with the different formulations to the respective models. When fitting the data to the Korsmeyer-Peppas model for burst effect, the release exponent (n) values obtained were 0.732, 0.860 and 1.000 for the nicotine-loaded nanofibers, lozenge and sublingual tablet, respectively. The value of n=1.000, obtained for the sublingual tablet is considered unreliable, due to the low R^2 value obtained for the respective data set ($R^2=0.753$). The obtained release constant values for data fitted to the Korsmeyer-Peppas model

for burst nicotine release ($n \geq 0.73$) from the nanofibers and from the lozenge indicated a non-Fickian and anomalous diffusion. This implies a release mechanism governed by more than one type of release phenomena; for example diffusion and swelling, or diffusion and erosion.[33,35] The 1st order release rate constant (k_1) and the Korsmeyer-Peppas rate constant (k_{KP}) were higher for the nicotine-loaded nanofibers than for the lozenge and the sublingual tablet. Application of the AIC demonstrated that the release data of the nicotine-loaded nanofibers fitted best to the 1st order kinetics model, whereas the release data of the lozenge and the sublingual tablet fitted best to the Hixson-Crowell release model. Furthermore, release data of the nicotine-loaded nanofibers was best fitted by the 1st order kinetics model, which is applicable for soluble drugs incorporated in a porous matrix and furthermore indicates that the amount of nicotine released remains proportional to the amount of nicotine remaining in the polymeric, porous matrix.[35] In contrast, the release of nicotine from the lozenge and the sublingual tablet was best fitted by the Hixson-Crowell release model, which suggests that the release from these two formulations is driven by diffusion with a minor effect of matrix dissolution/erosion.[33,48]

Table 2: Kinetic parameters, R^2 and AIC values obtained from fitting the 1st order kinetics, the Korsmeyer-Peppas model for burst effect and the Hixson-Crowell model to 60% of the obtained *in vitro* nicotine release data of the formulations tested: nicotine-loaded nanofibers, lozenge and sublingual tablet. The Hixson-Crowell model was only fitted to the release data of the lozenge and the sublingual tablet.

Formulation\Release model	1st order kinetics		Korsmeyer-Peppas for burst effect		Hixson-Crowell	
Nicotine-loaded nanofibers	k_1	0.063	k_{KP}	4.903	–	
			n	0.732		
	R^2	0.980	R^2	0.962	–	
	AIC	-8.795	AIC	25.902	–	
Lozenge	k_1	0.012	k_{KP}	1.065	k_{HC}	0.004
			n	0.860		
	R^2	0.936	R^2	0.973	R^2	0.999
	AIC	-19.319	AIC	13.801	AIC	-30.315
Sublingual tablet	k_1	0.025	k_{KP}	1.176	k_{HC}	0.007
			n	1.000		
	R^2	0.989	R^2	0.753	R^2	0.999
	AIC	-21.036	AIC	34.900	AIC	-33.781

Nicotine released from biocompatible nanofibers was transported across the buccal TR146 cell culture epithelium

The nanofibers were evaluated as a drug delivery system to facilitate the release and permeation of nicotine across the buccal epithelial barrier as demonstrated by a transport study using the human buccal epithelial TR146 cell culture model (Figure 4). The pH of the cell buffer was adjusted to a physiologically relevant pH of 6.8 (the average pH of saliva)[41] to counteract the decrease in pH induced by the bitartrate salt of NBT and potential undesired related effects on cell viability and epithelial integrity. Furthermore, controlling the pH was crucial as the permeation of nicotine depends on the degree of molecular ionization and thus pH.[7]

Neither the neat ALA/PEO nanofibers, the nicotine-loaded ALA/PEO nanofibers, nor nicotine in solution (0.3 mg/mL-corresponding to the theoretical concentration of nicotine released from a nicotine-loaded nanofiber disc) affected the viability of the TR146 cells compared to the buffer control (Figure 4A). Thus, good biocompatibility of the proposed drug delivery system was hereby demonstrated.

9.6±1.6% (N=3, n=3; mean ± SD) and 7.2±1.2% (N=3, n=2-3; mean ± SD) of the nicotine in solution and the nicotine in the nanofibers, respectively, was transported from the apical to the basal side of the TR146 cell layers within 3 h (Figure 4B). No notable difference was detected between the flux values of nicotine in solution with a concentration of 0.3 mg/mL and nicotine released from a nicotine-loaded ALA/PEO nanofiber disc; which were 0.73±0.17 nmol/(cm^2×min) (N=3, n=3; mean ± SD) and 0.6±0.11 nmol/(cm^2×min) (N=3, n=2-3; mean ± SD), respectively. This indicated that the permeability barrier was intact and not compromised by the presence of the nanofibers. The apparent permeability of the nicotine in solution was 6.6±1.6 ×10^{-6} cm/s (N=3, n=3; mean ± SD), which is in line with previously reported studies of nicotine permeation across the TR146 cell culture epithelium (P_{app}= 8.3±1.5 ×10^{-6} cm/s).[49] All samples applied to the cell culture model were isoosmolal (~300 mOsmol/kg). No notable differences were detected in the TEER before and after incubation, and the TEER were in the range 39-50 Ω×cm^2 for all samples evaluated. Hence, the epithelial integrity was maintained throughout the transport study.

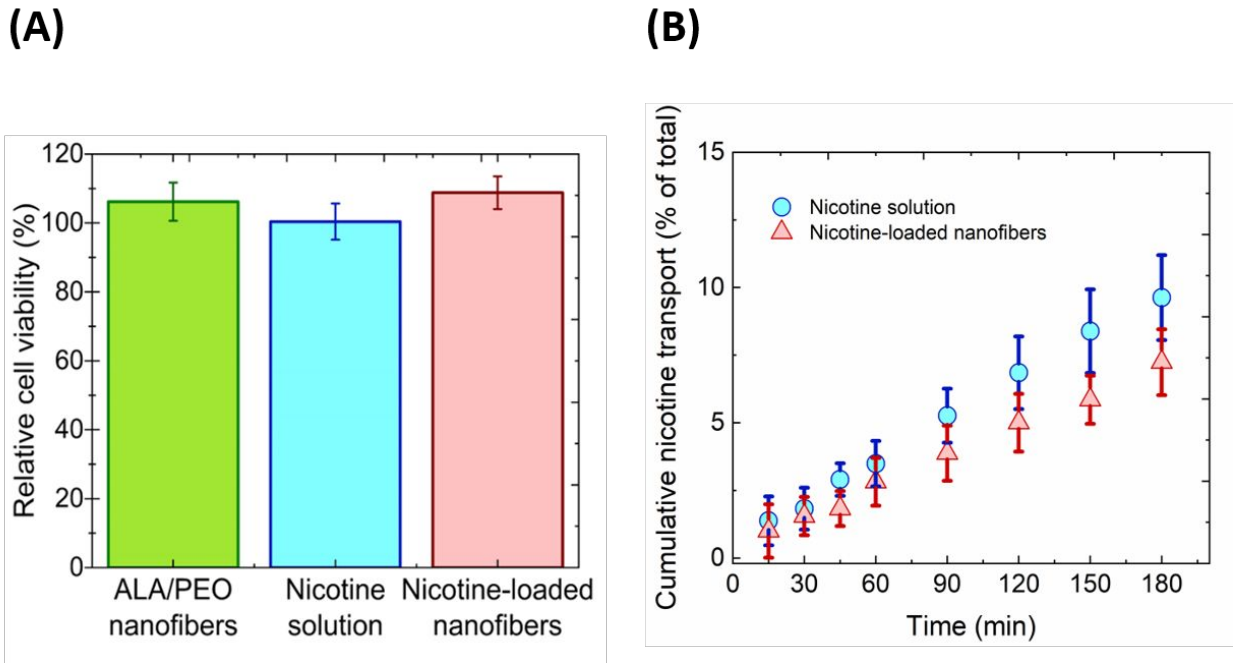

Figure 4: Nicotine transport across TR146 epithelium. (A) Cell viability (%) of filter-cultured TR146 cells exposed to neat ALA/PEO nanofibers (ALA/PEO nanofibers), 0.3 mg/mL nicotine in hHBSS (Nicotine solution) or nicotine-loaded ALA/PEO nanofibers (Nicotine-loaded nanofibers) relative to control (hHBSS). (B) Nicotine transport (% of total) from 0.3 mg/mL nicotine in hHBSS (Nicotine solution; 0.3 mg/mL equals to theoretical concentration of nicotine released from the nanofibers in hHBSS) and nanofiber disc with 0.225 mg deposited nicotine (Nicotine-loaded nanofibers), from the apical to the basal cell side of filter-cultured TR146 epithelium as a function of time during 3 h incubation. N=3, n=2-3, N representing the number of individual nanofiber mats prepared on separate days and individual cell passages, and n the number of samples from each replicate, results presented as the mean ± SD.

Ex vivo permeation of nicotine through porcine buccal mucosa

Permeation studies using *ex vivo* porcine buccal mucosa benefit from a relevant resemblance of histology of the human buccal mucosa, and that the submucosa and lamina propria is included in the barrier.[50] For comparative reasons, *ex vivo* porcine mucosa was exposed to an amount of nicotine in solution 10× higher than one dose provided by the nanofibers. Cumulative permeation of nicotine across the *ex vivo* porcine buccal mucosa after exposure to the nicotine-loaded ALA/PEO nanofibers or the solution of nicotine (Figure 5) resulted in flux values of 1.06±0.22 nmol/(cm^2×min) (N=3, n=2-3; mean ± SD) and only 0.17±0.14 nmol/(cm^2×min) (N=3, n=3; mean ± SD), respectively. For nicotine in solution, the apparent permeability was thus 4.00±3.25 ×10^{-8} cm/s (N=3, n=3; mean ± SD). Previous studies conducted for nicotine permeability through *ex vivo* porcine buccal mucosa with a thickness of 736±110 µm (n=4) reported apparent permeability values of 1.44±0.49 ×10^{-8} cm/s and 1.54±0.12 ×10^{-8} cm/s for nicotine in solutions of different

concentrations (10^{-2} M and 10^{-3} M, respectively) and at pH 7.4.[7] Noteworthy, the permeation of nicotine released from ALA/PEO nanofibers through *ex vivo* porcine buccal mucosa was not only more efficient than of a highly concentrated nicotine solution (10× the content of nicotine in the nanofibers), but also significantly faster (Figure 5). This could be attributed to the fact that the nicotine-loaded nanofibers were applied directly on the mucosa, providing fast nicotine release and a site-specific high nicotine concentration gradient across the mucosal tissue driving passive diffusion of nicotine into and through the buccal tissue.

Electrospun nanofibers have been employed to enable close contact between the epithelium of the oral mucosa and the released drug, especially if unidirectional release is ensured.[51] Backing layers, which are usually of hydrophobic nature, direct the potential drug release towards the mucosa, protect the releasing matrix against friction due to mechanical stress (movement of teeth and tongue) and protect from wash-out of drug by saliva and thus maintaining the concentration gradient for a prolonged time.[52] To simulate this, close contact between the nanofibers and the buccal mucosa and unidirectional release were assured during the *ex vivo* experiments. In general, the permeability of nicotine was higher across TR146 epithelium compared to that through *ex vivo* porcine buccal mucosa, which can mainly be explained by the increased thickness and higher barrier properties of the porcine buccal mucosa compared to the TR146 cell culture model.

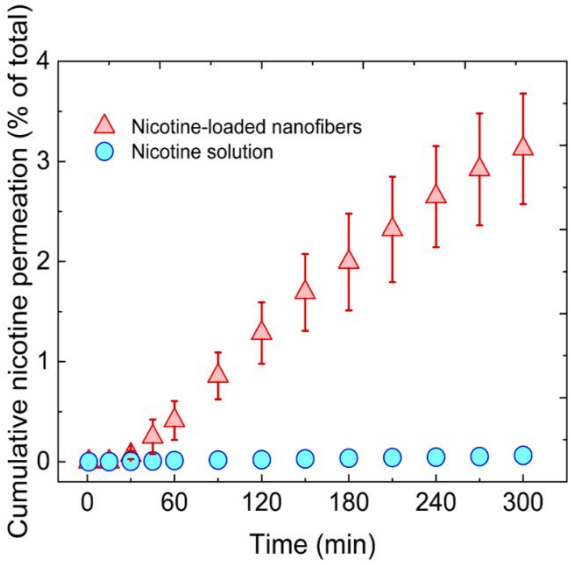

Figure 5: Permeation of nicotine through *ex vivo* porcine buccal mucosa. The permeated amount of nicotine (% of dose) from the donor compartment to the receptor compartment of the Ussing chambers given for *ex vivo* porcine buccal tissue exposed to nicotine-loaded nanofibers (Nicotine-loaded nanofibers) and nicotine in PBS of 5.625 mg/mL (Nicotine solution) as a function of

time during 5 h of incubation. N=3, n=2-3, N representing the number of replications (individual nanofiber mats, tissue obtained from individual pig), and n the number of individual samples tested. Results presented as mean ± SD for nicotine-loaded nanofibers and as mean values for nicotine solution. The SD bars for the nicotine solution are smaller than the symbol size.

Nicotine delivered from nanofibers penetrated efficiently into *ex vivo* buccal mucosa

MALDI MS imaging was conducted to assess the spatial distribution of nicotine into *ex vivo* porcine buccal mucosa after topical application of the nicotine-loaded ALA/PEO nanofibers. In Figure 6A, the spatial distribution of nicotine (*m/z* 162.123) is visualized in red and the epithelium is visualized in green by an endogenous molecule (sodium adduct of phosphatidylglycerol PG(34:1), *m/z* 771.5131). The relative nicotine distribution in tissue was also visualized without the epithelium biomarker (Figure 6B), using a color scale which provides a wider dynamic range than what is possible in the overlaid image. Remarkably, nicotine penetrated throughout the entire epithelium already within 1 h after the application of nicotine-loaded nanofibers on the *ex vivo* porcine buccal mucosa. Signals of low intensities of nicotine can even be observed in the lamina propria and the submucosa of the tissue, thus indicating penetration of nicotine also into these two regions after 1 h of exposure. This is in accordance with results of the *ex vivo* permeation study, which showed an approximate lag time of nicotine permeation through the *ex vivo* porcine mucosa of 30 min (Figure 5). Moreover, the most intense detection of nicotine occurred at the site of application of the nicotine-loaded nanofibers. H&E staining was conducted post MALDI MS imaging to evaluate the integrity of the tissue (Figure 6C). The tissue did not undergo visible damage after cutting, preparation and, most importantly, after exposure to the nicotine-loaded nanofibers for 1 h (Figure 6C). For comparison, MALDI MS imaging studies conducted by Marxen *et al.* (Figure 6D) suggest that the main permeability barrier to nicotine is located in the epithelium, since nicotine was not detectable further than the outer epithelial layers even after 3 h of apical exposure to nicotine in solution (61.6 mM corresponding to 10 mg/mL).[8] Overall, the permeation studies and supporting imaging clearly underline the efficiency of the nicotine-loaded ALA/PEO nanofibers as a fast-onset delivery system to facilitate the permeation of nicotine. The induced higher nicotine tissue penetration by dosing the nicotine in nanofibers thus highlights the importance of a tailored dosage form.

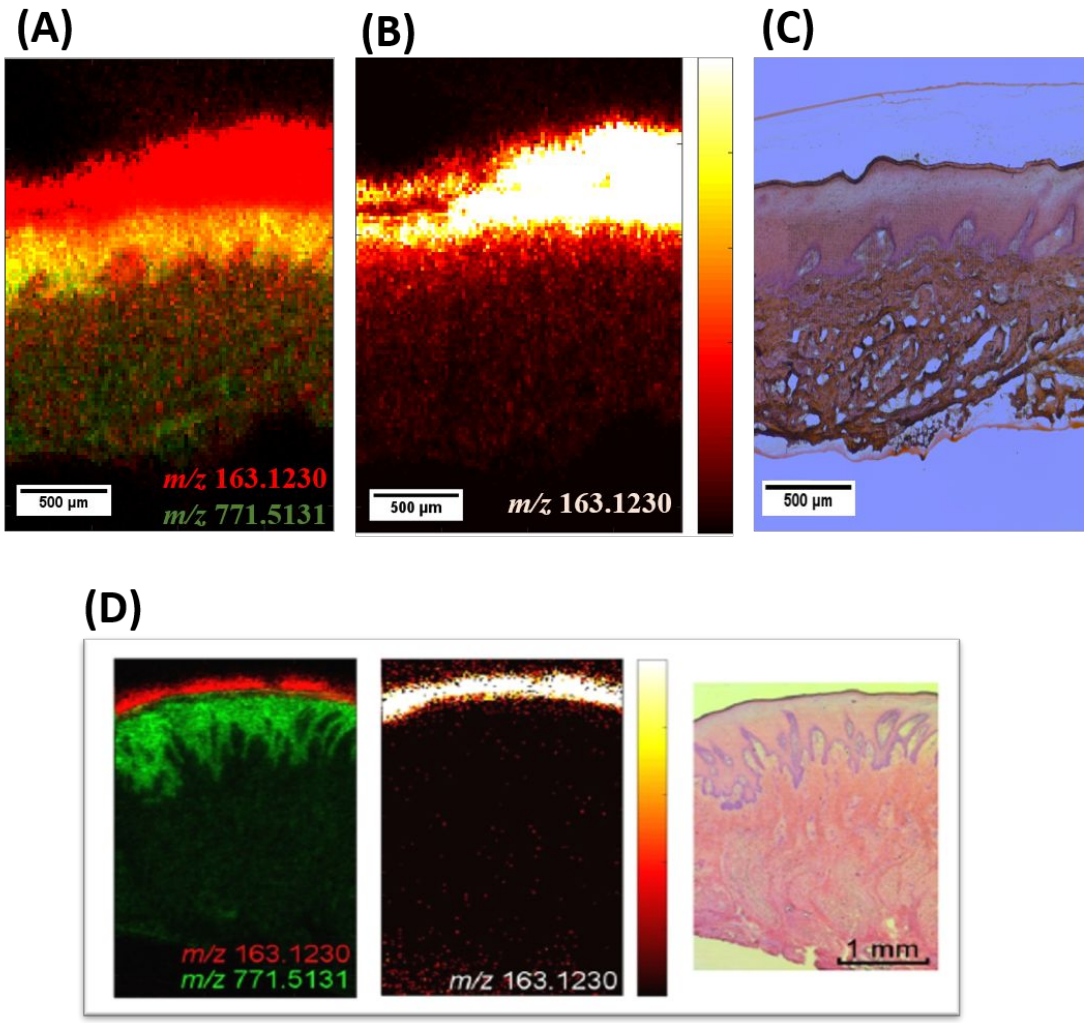

Figure 6: Representative images obtained by MALDI MS imaging of *ex vivo* porcine buccal mucosa exposed to nicotine-loaded nanofibers for 1 h. (A) MALDI MS overlay image of nicotine (red) and an epithelium tissue marker (green). Red: Nicotine, *m/z* 163.12297 $[M + H]^+$. Green: Epithelial marker PG (34:1), *m/z* 771.5131 $[M + Na]^+$. Spatial resolution: 20 µm. (B) Distribution of nicotine in *ex vivo* porcine buccal mucosa tissue, m/z 163.12297 $[M + H]^+$. Spatial resolution: 20 µm. The intensity color scale is shown next to the image. (C) H&E stained *ex vivo* porcine buccal mucosa after MALDI MS imaging. N=2, N representing the number of replicates (individual nanofiber mats and tissue obtained from individual pigs). (D) For comparison, MALDI MS and HE stained images of a cross section of porcine buccal mucosa apically exposed to 70 µL of 10 mg/mL nicotine in PBS for 3 h. Red: Nicotine, m/z 163.1230 $[M + H]^+$. Green: Epithelial marker PG (34:1), m/z 771.5131 $[M + Na]^+$. Spatial resolution was 20 µm. Adapted with permission from Marxen *et al.*.[8] Copyright (2018) American Chemical Society.

As previously reported, nicotine absorption across biological membranes is pH-dependent and nicotine penetrates the membranes faster in its unionized form.[5] Thus, to improve the absorption of nicotine, several of the existing NRT formulations, such as the nicotine chewing gum, are buffered to alkaline pH.[5] Accordingly, the permeation of nicotine released from the nanofibers

across buccal mucosa could potentially be further improved by the addition of buffering excipients to the nanofibers. Further, ensuring closer tissue contact by introducing mucoadhesive properties to the nicotine-loaded nanofibers, despite their fast disintegration, could enhance their effect. Overall, the present results support that nicotine released from the ALA/PEO nanofibers efficiently permeated the buccal absorption barrier. Their exceptional performance in promoting the mucosal permeation of nicotine as well as their superiority to marketed NRT formulations in terms of disintegration and nicotine release is expected to potentially satisfy cravings, omit throat soreness and inhibit relapse more efficiently than the existing oromucosal NRT formulations.

CONCLUSION

Nicotine was successfully loaded onto electrospun ALA/PEO nanofibers as a biocompatible drug delivery system for buccal administration. The loaded amount of nicotine onto the nanofibers was comparable to existing marketed oromucosal NRT formulations, namely a nicotine sublingual tablet and lozenge. Nicotine-loaded nanofibers demonstrated fast disintegration in aqueous medium and displayed the fastest release profile compared to two marketed NRT formulations for oromucosal administration. Nicotine released from ALA/PEO nanofibers permeated more efficiently through *ex vivo* porcine buccal tissue as compared to nicotine in solution. Increased tissue penetration was also verified by MALDI MS imaging of the spatial distribution of nicotine in *ex vivo* buccal tissue. Indeed, nicotine penetration into the epithelium, the lamina propria and the submucosa of the buccal tissue was achieved when nicotine-loaded ALA/PEO nanofibers were applied; this being an exceptional property of our drug delivery system. In conclusion, we show that ALA/PEO nanofibers can act as a biocompatible, site-specific and fast-releasing drug delivery system for nicotine and thus have potential to overcome the majority of drawbacks of already existing NRTs.

SUPPORTING INFORMATION

The file contains details on the procedure for nicotine deposition on the nanofibers and fitting of the release kinetics.

ACKNOWLEDGEMENTS

Authors acknowledge Davisco Food International/Agropur Ingredients (Eden Prairie, MN, USA) for providing α-lactalbumin. The Department of Experimental Medicine at the University of Copenhagen is greatly acknowledged for providing the porcine tissue used for the *ex vivo* studies. Charlotte Bagger is acknowledged for support with the MALDI-MS imaging studies and Lene Grønne Pedersen for conducting the cell cultivation.

Funding: VF and KK acknowledge the VILLUM FONDEN for the Villum Young Investigator Grant “Protein Superstructures as Smart Biomaterials (ProSmart)” 2018-2023 (project number: 19175). HMN, ISC, JJ, and MBS acknowledge The Danish Council for Independent Research; Technology and Production (DFF-6111-00333). HMN, VF, KK, and MBS acknowledge support from The Novo Nordisk Foundation for funding the Center for Biopharmaceuticals and Biobarriers

in Drug Delivery (Grand Challenge Program; NNF16OC0021948). Further, the Support from the Carlsberg Foundation and The Danish Council for Independent Research Medical Sciences (grant no. DFF – 4002-00391) is gratefully acknowledged.

AUTHORS CONTRIBUTION

VF, HMN, JJ, MBS developed the idea behind the project. VF, HMN, JJ, MBS, KK, and CJ designed the experiments. VF, HMN, JJ, CJ, and ISC provided the resources for the project. KK and MBS performed the experiments and analyzed the data. KK wrote the original draft. MBS, CJ, ISC, JJ, HMN, and VF reviewed and edited the manuscript. All authors approved the final version of the manuscript.

DECLARATION OF INTERESTS

The authors declare no conflict of interest.

REFERENCES

1. World Health Organization. WHO Report on the global tobacco epidemic. Geneva, 2019. https://apps.who.int/iris/bitstream/handle/10665/326043/9789241516204eng.pdf?ua=1 (accessed April 10, 2020).

2. U.S. National Cancer Institute and World Health Organization. *The Economics of tobacco and tobacco control; National Cancer Institute Tobacco Control Monograph 21*, NIH Publication No. 16-CA-8029A. Bethesda, MD: U.S. and Geneva, 2016; pp 65-99.

3. Cipolla D; Gonda I. Inhaled nicotine replacement therapy. *Asian J Pharm Sci*. **2015**, 10 (6), 472-480.

4. Vezina P; McGehee DS; Green WN. Exposure to nicotine and sensitization of nicotine-induced behaviors. *Prog Neuropsychopharmacol Biol Psychiatry* **2007**, *31* (8), 1625-1638.

5. Benowitz NL; Hukkanen J; Jacob P. Nicotine chemistry, metabolism, kinetics and biomarkers. *Handb Exp Pharmacol*. **2009**; *192*, 29-60.

6. National Center for Biotechnology Information. PubChem Database. Nicotine, CID=89594. https://pubchem.ncbi.nlm.nih.gov/compound/Nicotine (accessed April 10, 2020).

7. Nielsen HM; Rømer Rassing M. Nicotine permeability across the buccal TR146 cell culture model and porcine buccal mucosa in vitro: Effect of pH and concentration. *Eur J Pharm Sci*. **2002**, *16*, 151-157.

8. Marxen E; Jacobsen J; Hyrup B; Janfelt C. Permeability barriers for nicotine and mannitol in porcine buccal mucosa studied by high-resolution MALDI mass spectrometry imaging. *Mol Pharm*. **2018**, *15* (2), 519-526.

9. Prochaska JJ; Benowitz NL. The past, present, and future of nicotine addiction therapy. *Annu Rev Med*. **2016**, *67*, 467-486.

10. Aubin HJ; Luquiens A; Berlin I. Pharmacotherapy for smoking cessation: pharmacological principles and clinical practice. *Br J Clin Pharmacol*. **2014**, *77* (2), 324-336.

11. Dale MM; Rang HP; Flower RJ; Ritter JM. In *Rang and Dale's Pharmacol*ogy, 6th ed.; Churchill Livingstone: Edinburgh, 2007; pp 144-154.

12. Hartmann-Boyce J; Chepkin SC; Ye W; Bullen C; Lancaster T. Nicotine replacement therapy versus control for smoking cessation. *Cochrane Database Syst. Rev.* **2018**, *5* (5). https://doi:10.1002/14651858.CD000146.pub5.

13. West RJ. Psychology and pharmacology in cigarette withdrawal. *J Psychosom Res*. **1984**, *28* (5), 379-386.

14. Mills EJ; Wu P; Lockhart I; Wilson K; Ebbert JO. Adverse events associated with nicotine replacement therapy (NRT) for smoking cessation. A systematic review and meta-analysis of one hundred and twenty studies involving 177,390 individuals. *Tob Induc Dis*. **2010**, *8* (1). https://doi.org/10.1186/1617-9625-8-8.

15. Carpenter MJ; Jardin BF; Burris JL; Mathew AR; Schnoll RA; Rigotti NA, Cummings KM. Clinical strategies to enhance the efficacy of nicotine replacement therapy for smoking cessation: a review of the literature. *Drugs*. **2013**, *73* (5), 407-426.

16. Le Houezec J. Role of nicotine pharmacokinetics in nicotine addiction and nicotine replacement therapy: A review. *Int J Tuberc Lung Dis*. **2003**, *7* (9), 811-819.

17. Okeke OC; Boateng JS. Nicotine stabilization in composite sodium alginate based wafers and films for nicotine replacement therapy. *Carbohydr Polym*. **2017**; *155*, 78-88.

18. Boateng J; Okeke O. Evaluation of clay-functionalized wafers and films for nicotine replacement therapy via buccal mucosa. *Pharmaceutics*. **2019**; *11* (3). https://doi.org/10.3390/pharmaceutics11030104.

19. Tiffany ST; Cox LS; Elash CA. Effects of transdermal nicotine patches on abstinence-induced and cue-elicited craving in cigarette smokers. *J Consult Clin Psychol*. **2000**, *68* (2), 233-240.

20. Bruce C; Manning M, inventor; Novartis Ag, assignee. Melt extruded nicotine thin strips. Google Patent WO2011081628A1. 2009 Dec 30.

21. Silagy C; Lancaster T; Stead L; Mant D; Fowler G. Nicotine replacement therapy for smoking cessation. *Cochrane Database Syst Rev*. **2004**, *3*. https://doi:10.1002/14651858.CD000146.pub2.

22. Henningfield JE; Fant RV; Buchhalter AR; Stitzer ML. Pharmacotherapy for nicotine dependence. *CA Cancer J Clin*. **2005**, *55* (5), 281-299.

23. Khadka DB; Haynie DT. Protein- and peptide-based electrospun nanofibers in medical biomaterials. *Nanomedicine: Nanotechnology, Biology and Med*. **2012**, *8* (8), 1242-1262.

24. Babitha S; Rachita L; Karthikeyan K; Shoba E; Janani I; Poornima B; Sai P. Electrospun protein nanofibers in healthcare: A review. *Int J Pharm*. **2017**, *523*, 52-90.

25. Sullivan ST; Tang C; Kennedy A; Talwar S; Khan SA. Electrospinning and heat treatment of whey protein nanofibers. *Food Hydrocoll*. **2014**, *35*, 36-50.

26. Livney YD. Milk proteins as vehicles for bioactives. *Curr Opin Colloid Interface Sci*. **2010**, *15* (1-2), 73-83.

27. Stie MB; Corezzi M; Bombin ADJ; Ajalloueian F; Attrill E; Pagliara S; Jacobsen J; Chronakis IS; Mørck Nielsen H; Foderà V. Waterborne electrospinning of alpha-lactalbumin generates tunable and biocompatible nanofibers for drug delivery. *ACS Appl Nano Mater*. **2020**, *3* (2), 1910-1921.

28. Layman DK; Lönnerdal B; Fernstrom JD. Applications for α-lactalbumin in human nutrition. *Nutr Rev*. **2018**, *76* (6), 444-460.

29. Håkansson A; Svensson M; Mossberg AK; Sabharwal H; Linse S; Lazou I; Lönnerdal B; Svanborg C. A folding variant of a-lactalbumin with bactericidal activity against *Streptococcus pneumoniae*. *Mol Microbiol*. **2000**, *35* (3), 589-600.

30. Rammer P; Groth-Pedersen L; Kirkegaard T; Daugaard M; Rytter A; Szyniarowski P; Høyer-Hansen M; Klitgaard Povlsen L; Nylandsted J; Larsen JE; Jäättelä M. BAMLET activates a lysosomal cell death program in cancer cells. *Mol Cancer Ther*. **2010** *9* (1), 24-32.

31. Korhonen H. Bioactive Milk Proteins, Peptides and Lipids and Other Functional Components Derived from Milk and Bovine Colostrum. In *Functional Foods,* 2nd ed; Woodhead Publishing, 2011, pp 475-511.

32. Stie MB; Jones M; Sørensen HO; Jacobsen J; Chronakis IS; Mørck Nielsen H. Acids 'generally recognized as safe' affect morphology and biocompatibility of electrospun chitosan/polyethylene oxide nanofibers. *Carbohydr Polym*. **2019**, *215*, 253-262.

33. Mathematical models of drug release. In *Strategies to modify the drug release from pharmaceutical systems*.; Bruschi MLB Ed.; Woodhead Publishing, 2015; pp 63-86.

34. Zhang Y; Huo M; Zhou J; Zou A; Li W; Yao C; Xie S. DDSolver: an add-in program for modeling and comparison of drug dissolution profiles. *AAPS J*. **2010**, *12* (3), 263-271.

35. Costa P; Sousa Lobo JM. Modeling and comparison of dissolution profiles. *Eur J Pharm Sci*. **2001**, *13* (2), 123-133.

36. Marxen E; Axelsen MC; Pedersen AML; Jacobsen J. Effect of cryoprotectants for maintaining drug permeability barriers in porcine buccal mucosa. *Int J Pharm*. **2016**, *511* (1), 599-605.

37. Robichaud G; Garrard KP; Barry JA; Muddiman DC. MSiReader: an open-source interface to view and analyze high resolving power MS imaging files on Matlab platform. *J Am Soc Mass Spectrom*. **2013**, *24* (5), 718-721.

38. Janfelt C; Wellner N; Leger P-L; Kokesch-Himmelreich J; Hansen SH; Charriaut-Marlangue C; Hansen HS. Visualization by mass spectrometry of 2-dimensional changes in rat brain lipids, including N -acylphosphatidylethanolamines, during neonatal brain ischemia. *FASEB J*. **2012**, *26* (6), 2667-2673.

39. Santocildes-Romero ME; Hadley L; Clitherow KH; Hansen J; Murdoch C; Colley HE; Thornhill MH; Hatton PV. Fabrication of electrospun mucoadhesive membranes for therapeutic applications in oral medicine. *ACS Appl Mater interfaces*, **2017**, *9* (13), 11557-11567.

40. National Center for Biotechnology Information. PubChem Database. Bitartrate, CID=3667129. https://pubchem.ncbi.nlm.nih.gov/compound/Bitartrate (accessed July 7, 2019).

41. Aframian D; Davidowitz T; Benoliel R. The distribution of oral mucosa pH values in healthy saliva secretors. *Oral Dis*. **2006**, *12* (4), 420-423.

42. Torres-Martinez EJ; Cornejo Bravo JM; Serrano Medina A; Pérez González GL; Villarreal Gómez LJ. A summary of electrospun nanofibers as drug delivery system:drugs loaded and biopolymers used as matrices. *Curr Drug Deliv*. **2018**, *15* (10), 1360-1374.

43. Um-i-Zahra S; Zhu L. Novel drug loaded duplicate nanofibers and their in vitro drug release profiles. *Am Res Thoughts*, **2015**, *1* (6), 1683-1698.

44. Aguilar Z.Targeted drug delivery. In *Nanomaterials for Medical Applications*; Elsevier Inc. 2013; pp 181-234.

45. Li X; Kanjwal MA; Lin L; Chronakis IS. Electrospun polyvinyl-alcohol nanofibers as oral fast-dissolving delivery system of caffeine and riboflavin. *Colloids Surfaces B Biointerfaces*, **2013**, *103*, 182-188.

46. Caplan JL, inventor; Caplan JL, assignee. New therapeutic method of delivering a medicament to avoid irritating effects on membranes of users. International Patent WO2003077846A2. 2003 Sep 25.

47. Gajendran J; Kraemer J; Knudsen Randers S. Product performance test for medicated chewing gums. *Dissolution Techn.* **2008**, *17* (3), 15-18.

48. Derakhshandeh K; Erfan M; Dadashzadeh S. Encapsulation of 9-nitrocamptothecin, a novel anticancer drug, in biodegradable nanoparticles: Factorial design, characterization and release kinetics. *Eur J Pharm Biopharm*., **2007**, *66* (1), 34-41.

49. Marxen E; Mosgaard MD; Pedersen AML; Jacobsen J. Mucin dispersions as a model for the oromucosal mucus layer in in vitro and ex vivo buccal permeability studies of small molecules. *Eur J Pharm Biopharm*. **2017**, *121*, 121-128.

50. Pinto S; Pintado ME; Sarmento B. In vivo, ex vivo and in vitro assessment of buccal permeation of drugs from delivery systems. *Expert Opin Drug Deliv*. **2020**, *17* (1), 33-48.

51. Colley HE; Said Z; Santocildes-Romero ME; Baker SR; Apice KD; Hansen J; Siim Madsen L; Thornhill MH; Hatton PV; Murdoch C. Pre-clinical evaluation of novel mucoadhesive bilayer patches for local delivery of clobetasol-17-propionate to the oral mucosa.

Biomaterials, **2018**, *178*, 134-146.

52. Chinna Reddy P; Chaitanya KS; Madhusudan Rao Y. A review of bioadhesive buccal drug delivery systems: current status of formulation and evaluation methods. Daru, **2011**, *19* (6), 385-403.

GRAPHICAL ABSTRACT

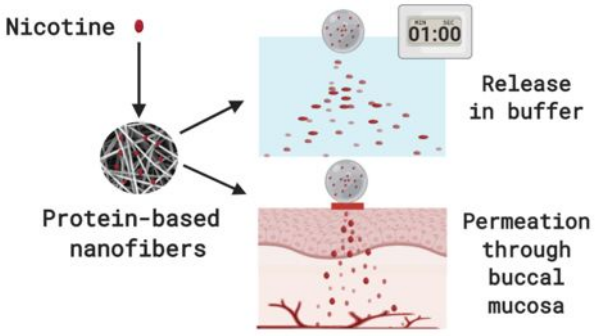

Graphical abstract for "Electrospun α-lactalbumin nanofibers for site-specific and fast-onset delivery of nicotine in the oral cavity: an *in vitro*, *ex vivo* and tissue spatial distribution study." Created with BioRender.com.